NJC

Accepted Manuscript

This is an *Accepted Manuscript*, which has been through the Royal Society of Chemistry peer review process and has been accepted for publication.

Accepted Manuscripts are published online shortly after acceptance, before technical editing, formatting and proof reading. Using this free service, authors can make their results available to the community, in citable form, before we publish the edited article. We will replace this *Accepted Manuscript* with the edited and formatted *Advance Article* as soon as it is available.

You can find more information about *Accepted Manuscripts* in the Information for Authors.

Please note that technical editing may introduce minor changes to the text and/or graphics, which may alter content. The journal's standard Terms & Conditions and the Ethical guidelines still apply. In no event shall the Royal Society of Chemistry be held responsible for any errors or omissions in this *Accepted Manuscript* or any consequences arising from the use of any information it contains.

ROYAL SOCIETY OF CHEMISTRY

www.rsc.org/njc

Charge transfer complexes of 4-isopropyl-2-benzyl-1,2,5-thiadiazolidin-3-one1,1-dioxide with DDQ and TCNE : Experimental and DFT studies

Saida Seridi [1], Karim Dinar[1], Achour Seridi [1], Malika Berredjem [2] and Mekki Kadri[1*]

[1] Laboratoire de Chimie Physique, Université 08 Mai 1945, BP401, Guelma 24000, Algeria.

[2] Laboratoire de Chimie Organique Appliquée, Groupe de Chimie Bioorganique.
Université Badji-Mokhtar, Annaba, BP 12, Algeria.

Abstract

The charge transfer complexes of the donor 4-isopropyl-2-benzyl-1,2,5-thiadiazolidin-3-one1,1-dioxide (SF) with the π acceptors 2,3-dichloro-5,6-dicyano-1,4-benzoquinone (DDQ) and tetracyanoethylene (TCNE) have been studied spectrophotometrically in chloroform and methanol at room temperature. The results indicated the formation of CT-complexes with molar ratio1:1 between donor and each acceptor at maximum CT-bands. The physical parameters of the CT-complexes were evaluated by the Benesi–Hildebrand equation. The data were analyzed in terms of their stability constant (K), molar extinction coefficient (ε_{CT}), thermodynamic standard reaction quantities (ΔG^0, ΔH^0, ΔS^0), oscillator strength (f), transition dipole moment (μ_{EN}) and ionization potential (I_D). The experimental studies were complemented by quantum chemical calculations by the Time-Dependent Density Functional Theory (TD-DFT) at B3LYP level.

The theoretical UV visible and FT-IR spectra were compared with those obtained experimentally. The first order hyperpolarizability (β_0) and related properties (α_0 and $\Delta\alpha$) are calculated using B3LYP method on the finite-field approach. The Mulliken charges, MEP calculations, the electronic properties HOMO and LUMO energies and NBO analysis were performed on optimized charge transfer complex SF-DDQ.

Key words: Sulfahydantoins; Charge-transfer complexes; TD-DFT; HOMO-LUMO; Mulliken charges ; MEP.

* Corresponding author.
Tel.: +213 772749499. E-mail address: mekkadri@gmail.com(M. Kadri).

New Journal of Chemistry Accepted Manuscript

1. Introduction

Non-covalent interactions, such as hydrogen bonds, π-π stacking, electrostatic and hydrophobic interactions, are ubiquitous in biological systems [1]. Their inherent reversibility makes them also interesting for technological applications such as stimulus-responsive surfaces and molecular recognition. One of these non-covalent interactions is the charge-transfer (CT) interaction. Molecular charge-transfer complexes are based on the interaction between two molecular species, namely donor (D) and acceptor (A). The donor molecule has small ionization energy (IP), while the counterpart acceptor molecule has a large electronegativity or electron affinity (EA). When donor and acceptor interact, the charge is redistributed among the compound. The CT interaction is often evidenced by the appearance of a characteristic absorption band in the visible spectrum. The CT interaction play an important role in biological systems like DNA binding, antibacterial, antifungal, insecticide, in ion transfer through lipophilic membranes [2-9]. Charge transfer complexes are currently of great importance since these materials can be utilized as organic semiconductors [10] and photo catalysts [11]. The charge transfer complexes formed in the reaction of electron acceptors with donors containing nitrogen, sulfur, oxygen atoms have attracted considerable attention and growing importance in recent years [12–17].

The introduction of the sulfamido group –NH–SO_2–NH– into a heterocyclic structure can lead to interesting new chemical and/or pharmacological potentialities [18]. Thus sulfahydantoins (3-oxo-1,2,5-thiadiazole-1,1-dioxides) (Fig.1) constitute as an emergent class of heterocycles, claimed as protease inhibitors (especially matrix proteinases) and ligand of MHC class II [19-23], aglygones in pseudonucleoside analogues [24], phosphate mimetic [25], or substructure in the constrained peptides [26]. In addition sulfahydantoins have been investigated as antihypertensives [27], artificial sweeteners [28], and histamine H_2-receptor antagonists [29].

This paper presents studies of the charge-transfer interaction between one sulfahydantoin : 4-isopropyl-2-benzyl-1,2,5-thiadiazolidin-3-one1,1-dioxide (SF) and DDQ or TCNE as π-acceptors (Fig.1). The donor molecule used in this study was, an aromatic heterocyclic compound representing a very important class of compounds which possess a system of π- and n-electrons.

New Journal of Chemistry Accepted Manuscript

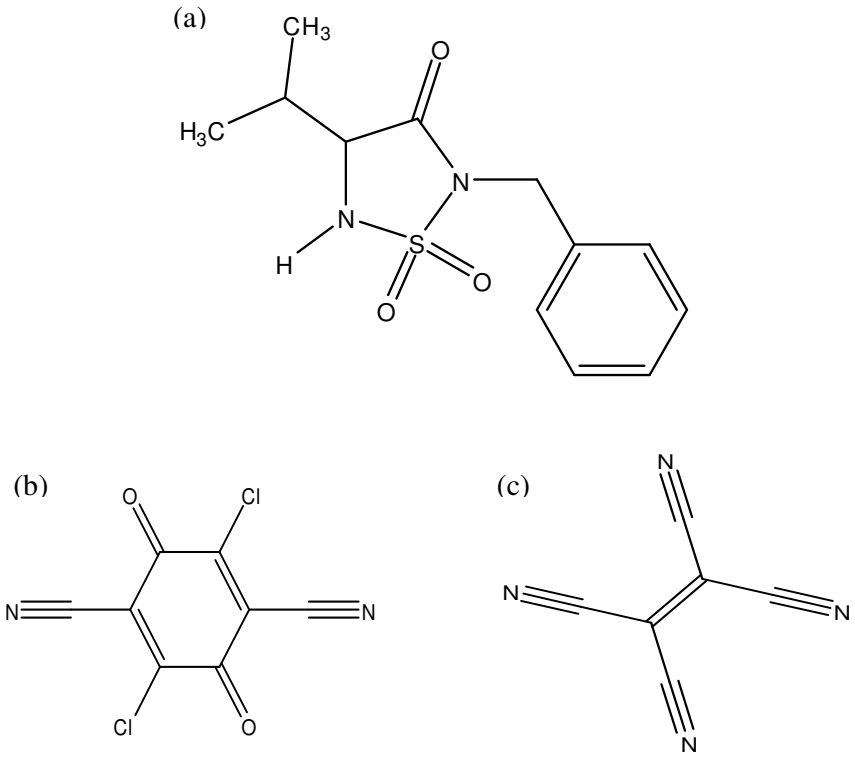

Fig.1 Structures of SF (a), (DDQ) (b) and (TCNE) (c).

The objective of the first aspect of this study is to carry out spectroscopic and thermodynamic studies of the complexation of the donor and the acceptors following two procedures: in liquid phase and at the solid state.

Spectrophotometric measurements in two solvents with distinct dielectric constants (chloroform (4.8), and methanol (32.7)), were used to evaluate stability constants (K), the molar extinction coefficient (ε_{CT}), thermodynamic standard reaction quantities ($\Delta G^0, \Delta H^0, \Delta S^0$), the oscillator strength (f), the transition dipole moment (μ_{EN}) and the ionization potential (I_D). The solid complexes were synthesized and characterized by using FT-IR spectroscopy.

In the second part of this work, we report the results from DFT and TD-DFT calculations on the SF-DDQ complex, the Mulliken charges, MEP calculations, the electronic properties HOMO and LUMO energies and NBO analysis were performed on the optimized charge transfer complex. The theoretical UV visible and FTIR spectra were compared with those obtained experimentally.

New Journal of Chemistry Accepted Manuscript

2. Experimental

2.1. Materials and instrumentation

All chemicals used were of high grade. SF was synthesized according to literature [30]. π-acceptors tetracyanoethylene (TCNE), and 2,3-dichloro-5,6-dicyano-1,4-benzoquinone (DDQ) were obtained from Aldrich Chemical Co. and were used without modification. The spectroscopic grade solvents (chloroform and methanol) were purchased from Fluka or Prolabo. The electronic absorption spectra were recorded in the range 400–220 nm using a Jasco UV-Vis. V530 spectrophotometer equipped with a Jasco EHC-477S thermostat (±0.1 °C) using 1.0 cm matched quartz cells. FT-IR spectra of the reactants and the formed complexes were recorded as KBr pellets using Spectrum one Perkin Elmer FT-IR.

2.2. Preparation of the solid complexes

The solid charge-transfer complexes were isolated by taking equimolar amounts of the donor and the acceptor and dissolved separately at room temperature in the minimum volume of a mixture methanol/dichloromethane (1:1, v/v). The two solutions were mixed and the resulting mixture was stirred overnight at room temperature. The resulting solid compound precipitated was first filtered off, washed several times with methanol/dichloromethane mixture to remove any unreacted materials, and finally dried.

2.3. Computational details

The Gaussian 09 program [31] was used for the Density Functional Theory (DFT) calculation of the complex in gas phase. The geometries of the complexes were optimized at the Becke's three parameter hybrid method with LYP correlation (B3LYP) [32–35]. 6-311G (d,p) basis set was used for optimization of SF, DDQ and SF**…**DDQ complex. In addition to optimization, Time-Dependent Density Functional Theory (TD-DFT) was also done at same B3LYP level of calculation in PCM model, using chloroform as a solvent. The electronic properties such as HOMO and LUMO energies were determined by DFT approach.

3. Results and discussion

3.1. Electronic spectra

The electronic absorption spectra of SF in solutions containing various amounts of DDQ or TCNE in chloroform are shown in Figs 2 and 3.

Fig. 2 shows electronic absorption spectra of SF in chloroform containing various concentrations of DDQ. The recorded spectra were detected real absorption bands which do

New Journal of Chemistry Accepted Manuscript

not existed in both spectra of the free donor and acceptors. These bands are noticed at 263 and 353 nm. These findings indicate the formation of a charge-transfer complex of SF with DDQ.

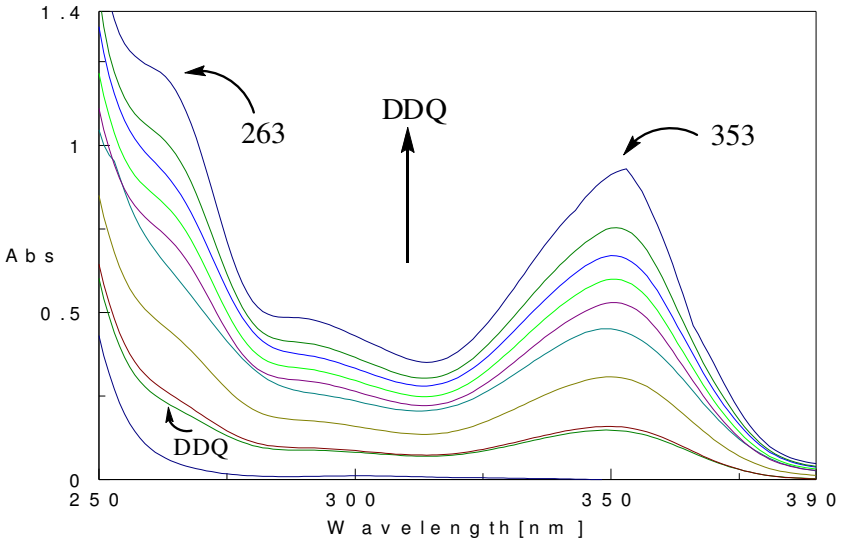

Fig. 2 Absorption spectra of SF (4×10^{-4} M) in chloroform containing various concentrations of DDQ.

Fig. 3 displays absorption spectra of SF in chloroform with progressive concentrations of TCNE. As the TCNE concentration increases, the absorbance at 264 nm enhances and a new absorption band at 276 nm appears which is clearly due to the charge-transfer complex.

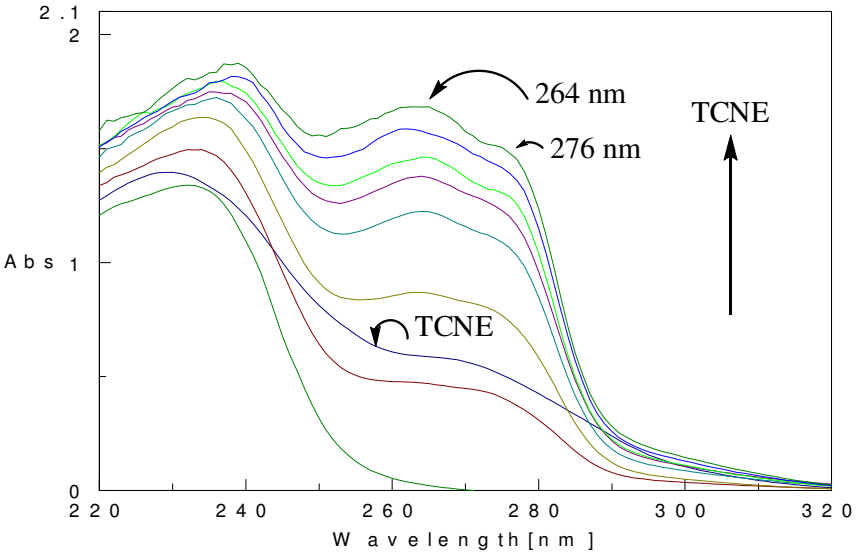

Fig. 3 Absorption spectra of SF (4×10^{-4} M) in chloroform containing various concentrations of TCNE.

New Journal of Chemistry Accepted Manuscript

3.2. Stoichiometric of CT complexes

The stoichiometry of the CT complexes formed between SF and π- acceptors was determined by Job's continuous variation method using absorption data [36].

The experiments use stock solutions with equimolecular concentrations of donor and acceptor components. The samples are prepared by mixing different volumes of these two solutions in such a way that the total concentration [donor]+[acceptor] remains constant and the molar fraction of the donor varies in the range 0–1 [37].

Interestingly, the donor acceptor molar ratio was found 1:1 for all complexes, as shown in figures 4-5.

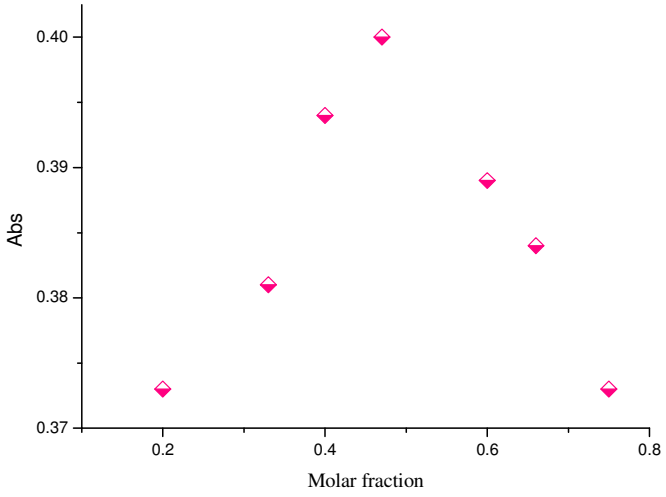

Fig. 4 Continuous variation plot for charge-transfer reaction in chloroform between DDQ as acceptor and SF as donor.

New Journal of Chemistry Accepted Manuscript

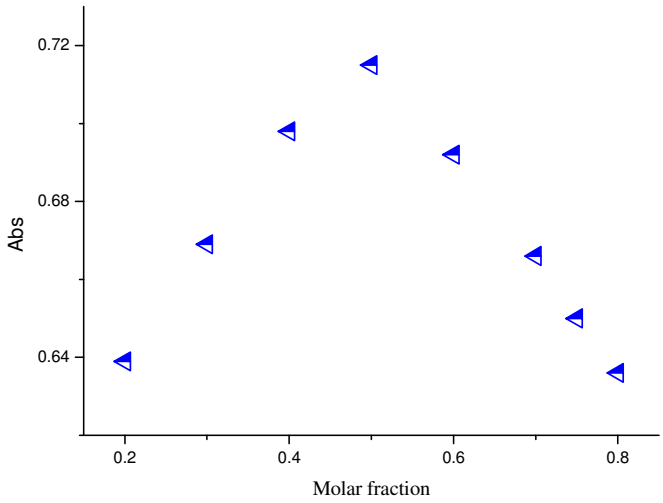

Fig. 5 Continuous variation plot for charge-transfer reaction in chloroform between TCNE as acceptor and SF as donor.

3.3. Determination of the composition of the complexes and their stability constants

The Benesi–Hildebrand equation (1) [38] was used to calculate the values of the stability constants K, and the extinction coefficients ε_{CT} for the complexes:

$$\frac{C_a^0 C_d^0}{Abs} = \frac{1}{K\varepsilon_{CT}} + \frac{C_d^0}{\varepsilon_{CT}} \qquad (1)$$

Where C_a^0 and C_d^0 are the initial concentrations of the acceptors (DDQ, and TCNE) and the donor (SF), respectively. Abs is the absorbance of CT complex. $C_a^0 . C_d^0$/Abs values for each system were plotted against to the corresponding (C_d^0) values. Straight lines were obtained with a slope of $1/\varepsilon_{CT}$ and intercept of $1/K\varepsilon_{CT}$, for the reaction of SF and DDQ in chloroform at 25°C as shown in (fig.6). K is the stability constant of the complex. Eq.(1) is valid under the condition $C_d^0 >> C_a^0$.

The Benesi–Hildebrand [38,39] method is an approximation that has been used many times and gives decent results. But the extinction coefficient is really a different one between the complex and free species that absorbs at the same wavelength. In all systems very good linear plots according to Eq.(1) [38,39] are obtained (Fig.6).

New Journal of Chemistry Accepted Manuscript

The values of K and ε_{CT} associated with all complexes are reported in Table 1.

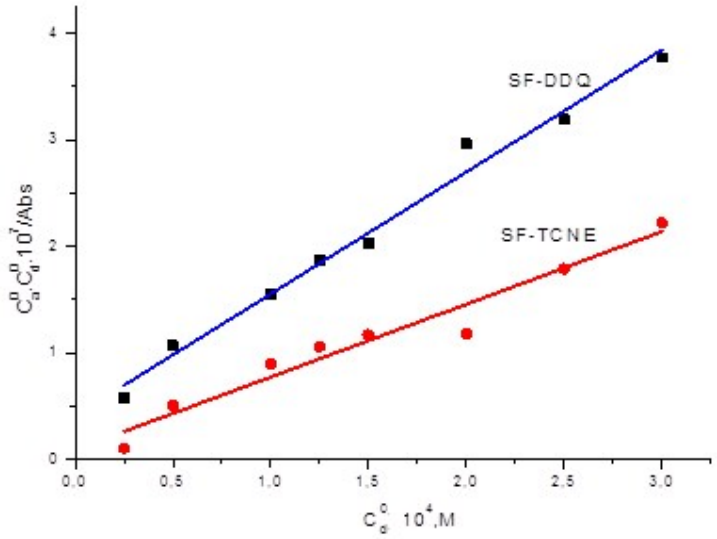

Fig. 6 Benesi Hildebrand plot for SF…DDQ and SF…TCNE complexes in chloroform at 25°C.

Table.1 Stability constants K and molar extinction coefficients ε_{CT} at 25°C of 1:1 SF-acceptors complexes.

Complexes	**Solvent**	**λ_{CT} (nm)**	**K × 10^{-3}**	**$\varepsilon_{CT} \times 10^{-3}$, L.mol^{-1}.cm^{-1}**
SF…DDQ	Chloroform	263	27.70	0.87
		353	29.40	7.90
SF…TCNE		264	40.43	0.39
		276	41.60	1.51
SF…DDQ	Methanol	246	8.59	0.40
SF…TCNE		238	6.07	2.95

As expected, the stability constants in chloroform were higher than those in methanol since it's known that the CT complex is stabilized in less polar solvent [40] and that the dissociation of the complex into $D^+ - A^-$ radicals has been found to occur in the ground state [41].

New Journal of Chemistry Accepted Manuscript

3.4. Determination of thermodynamic parameters of CT complexes

Thermodynamic parameters such as enthalpy change (ΔH^0), entropy change (ΔS^0) and free energy change (ΔG^0) of the complexation reaction were determined from the van't Hoff plot (Fig.7) [42, 43]. The temperature dependence of the stability constant was studied at different temperatures (288, 293, 298 and 303 K). The thermodynamic parameters were evaluated using the following equation:

$$\ln K = -\frac{\Delta H^0}{RT} + \frac{\Delta S^0}{R} \qquad (2)$$

A plot of $\ln K$ vs. 1/T for the studied charge-transfer complexes is shown in Fig.7. The enthalpies and entropies of complexation were determined from the slopes and intercepts, respectively.

The values of standard free energy changes were obtained according to the equation:

$$\Delta G^0 = \Delta H^0 - T\,\Delta S^0 = -RT\ln K \qquad (3)$$

Where K and R are the stability, and gas constants, respectively. The Calculated thermodynamic parameters from the van't Hoff plot using the above mentioned equations are listed in Table 2.

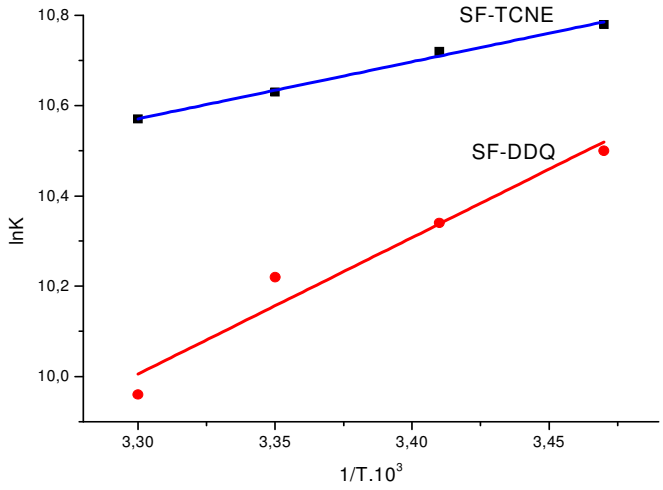

Fig. 7 Van't Hoff plots of the complex of DDQ and TCNE with SF in chloroform.

New Journal of Chemistry Accepted Manuscript

Table.2 Thermodynamic standard reaction quantities of SF complexes with DDQ and TCNE in different solvents.

Complexes	Solvent	ΔG^0 (kJ/mol)	ΔH^0 (kJ/mol)	ΔS^0 (J/K.mol)
SF…DDQ	Chloroform	-25.2	-28.3	-10.38
SF…TCNE		-26.2	-10.4	53.18
SF…DDQ	Methanol	-22.4	-25.6	-10.47
SF…TCNE		-21.6	-9.25	41.55

The values of thermodynamic parameters listed in Table 2 show that the charge-transfer reactions are exothermic, and are all thermodynamically favored $\left(\Delta G^0 \langle 0\right)$.

3.5. Determination of ionization potentials of the donor

The ionization potentials of the donor (ID) in the charge-transfer complexes were calculated using the empirical equation derived by Aloisi and Pignataro [44]:

I_D (eV) = 5.76 + 1.53 × 10^{-4} ν_{CT} for DDQ (4)

I_D (eV) = 5.21 + 1.65 × 10^{-4} ν_{CT} for TCNE (5)

Where ν_{CT} is the wavenumber in cm^{-1} of the complex, which was determined in each solvent. The determined values of ionization potentials are given in Table 3.

3.6. Determination of oscillator strength (f) and transition dipole moment (μ_{EN})

The experimental oscillator strength (f), which is a dimensionless quantity, used to express the transition probability of the CT-band [45] and transition dipole moment (μ_{EN}) of the formed complex [46] were calculated through the following equations [47]:

$$f = 4.32 \times 10^{-9} \int \varepsilon_{CT} d\nu \qquad (6)$$

Where $\int \varepsilon_{CT} d\nu$ is the area under the curve of the molar extinction coefficient of the absorption band in question vs. frequency. As a first approximation:

$$f = 4.32 \times 10^{-9}\ \varepsilon_{CT} \Delta\nu_{1/2} \qquad (7)$$

Where ε_{CT} is the maximum extinction coefficient of the band and $\Delta\nu_{1/2}$ is the half-width, i.e., the width of the band at half the maximum extinction. The values of the calculated oscillator

New Journal of Chemistry Accepted Manuscript

strengths indicate a strong interaction between the donor–acceptor pair with relative high probabilities of CT transitions. This is also supported by the relatively large heat formation.

The extinction coefficient is related to the transition dipole by:

$$\mu_{EN} = 0.0952\left[\varepsilon_{CT}\Delta\nu_{1/2} / \Delta\nu\right]^{1/2}$$

Where $\Delta\nu \approx \nu_{CT}$ at ε_{CT} and μ_{EN} is defined as $-e\int \Psi_{ex}\sum_i r_i \Psi_g d\tau$

The observed oscillator strengths of the CT bands and transition dipole are summarized in Table 3

Table.3 Spectral properties of CT complexes of SF with DDQ and TCNE in Chloroform and methanol.

Complexes	**Solvent**	**λ_{CT} (nm)**	I_D (eV)	f	μ_{EN} (D)
SF…DDQ	Chloroform	263	11.58	3.58	2.38
		353	10.10	10.95	1.07
SF…TCNE		264	11.46	2.10	3.13
		276	11.18	9.16	3.69
SF…DDQ	Methanol	246	11.98	1.15	1.57
SF…TCNE		238	12.14	6.40	1.13

3.7. FT-IR spectra

The FT-IR spectra bands of free donor (SF), free acceptors (DDQ, TCNE), and of their corresponding charge-transfer complexes are shown in (Figs.8 and 9), while the assignments of their characteristic FT-IR spectral bands are reported in Tables 4 and 5.

The formation of CT-complexes during the reaction of SF with DDQ or TCNE is strongly supported by observing of main infrared bands of the donor (SF) and acceptors (DDQ, TCNE) in the product spectra. These new bands undergo more or less important shifts in wavenumbers values and /or variation in signals intensities compared with those of the free donor and acceptors. For example, the vibration frequency of the C ≡ N group for free DDQ observed at 2254 cm^{-1} is shifted to 2250 cm^{-1} in the IR spectrum of the CT complex. Also, free TCNE shows one $\nu_{C\equiv N}$ vibration at 2220 cm^{-1} while in the complex it moved to 2224 cm^{-1}. In addition, it was also noticed that in both cases the observed $\nu_{C\equiv N}$ signal decreases in intensity.

New Journal of Chemistry Accepted Manuscript

The stretching vibration of the amine group is appeared at 3309 cm^{-1} for free SF compared with 3312 and 3310 cm^{-1} for the SF**…**DDQ and SF**…**TCNE complexes, respectively.

Interestingly, upon the complexation, the characteristic band of C=C observed at 1499, 1555 and 1511cm^{-1} in the free SF, free DDQ and free TCNE, respectively, is affected in intensity and shifted to 1454 cm^{-1} in SF**…**DDQ, and to 1593 cm^{-1} in SF**…**TCNE complexes. These findings, it may be concluded that the molecular complex is formed through n-π* and π-π* charge migration from HOMO of the donor to the LUMO of the acceptor [48]. The assumption of the interaction through π-π* transition is confirmed by the involving of the vibration frequency of C=C bands from two complexes (Scheme 1).

Table.4 Characteristic infrared[a] frequencies (cm^{-1}) and tentative assignments for SF, DDQ and their complex.

DDQ	**SF**	**DDQ…SF**	**Assignements**
-	3309s	3312m	ν_{N-H}
-	2961w	2962w	ν_{C-H}
2254m	-	2250w	$\nu_{C\equiv N}$
1698m 1676m	1732s	1735s	$\nu_{C=O}$
1555m	1499m	1454w	$\nu_{C=C}$
-	1326m	1351m	ν_{SO_2}
1276m	1274m	1281m	ν_{C-N}
-	1470m	1455m	δ_{C-H}
1193m 1174m	1174m	1175m	ν_{C-O}
887m	-	889m	ν_{C-Cl}

[a] s, strong; w, weak; m, medium; br, broad

New Journal of Chemistry Accepted Manuscript

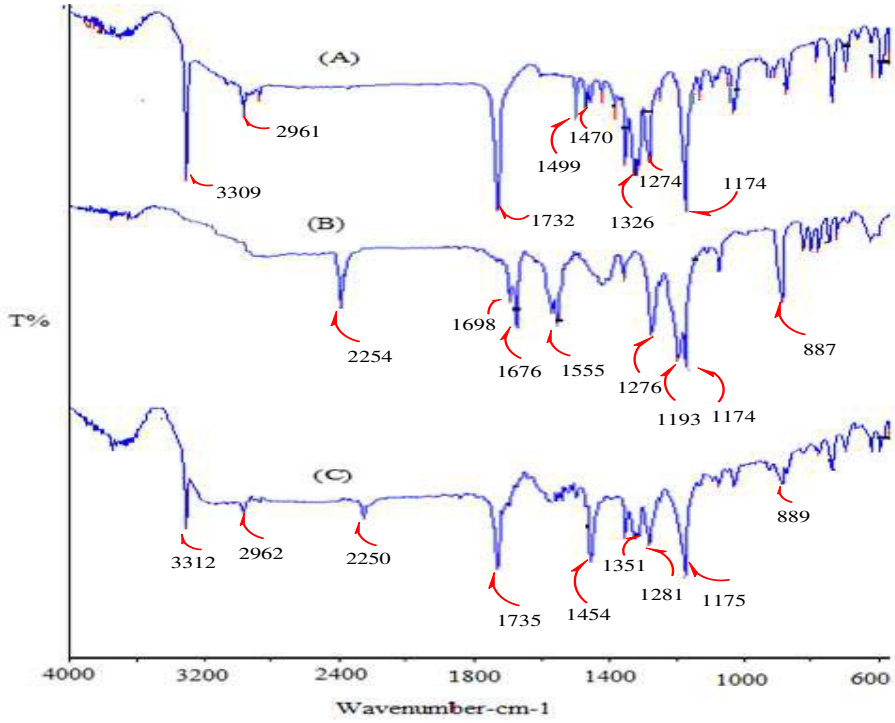

Fig. 8 FT-IR of free donor (A), the free DDQ (B), and their corresponding charge-transfer complex (C).

Table.5 Characteristic infrared[a] frequencies (cm^{-1}) and tentative assignments for SF, TCNE and their complex.

TCNE	SF	TCNE…SF	Assignements
-	3309s	3310m	ν_{N-H}
-	2961w	2962w	ν_{C-H}
2258s 2220s	-	2224m	$\nu_{C\equiv N}$
-	1732s	1737s	$\nu_{C=O}$
1511w	1499m	1593m	$\nu_{C=C}$
-	1326m	1351m	ν_{SO_2}
1146s	1274s	1283s	ν_{C-N}
-	1470m	1471m	δ_{C-H}
-	1174m	1177m	ν_{C-O}

New Journal of Chemistry Accepted Manuscript

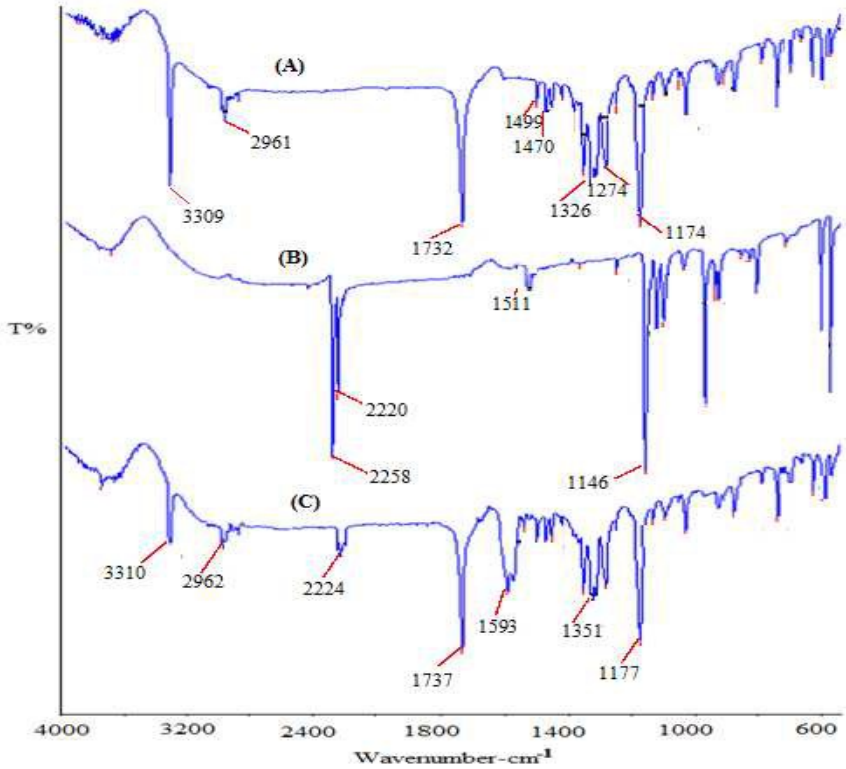

Fig. 9 FT-IR of free donor (A), the free TCNE (B), and their corresponding charge-transfer complex (C).

New Journal of Chemistry Accepted Manuscript

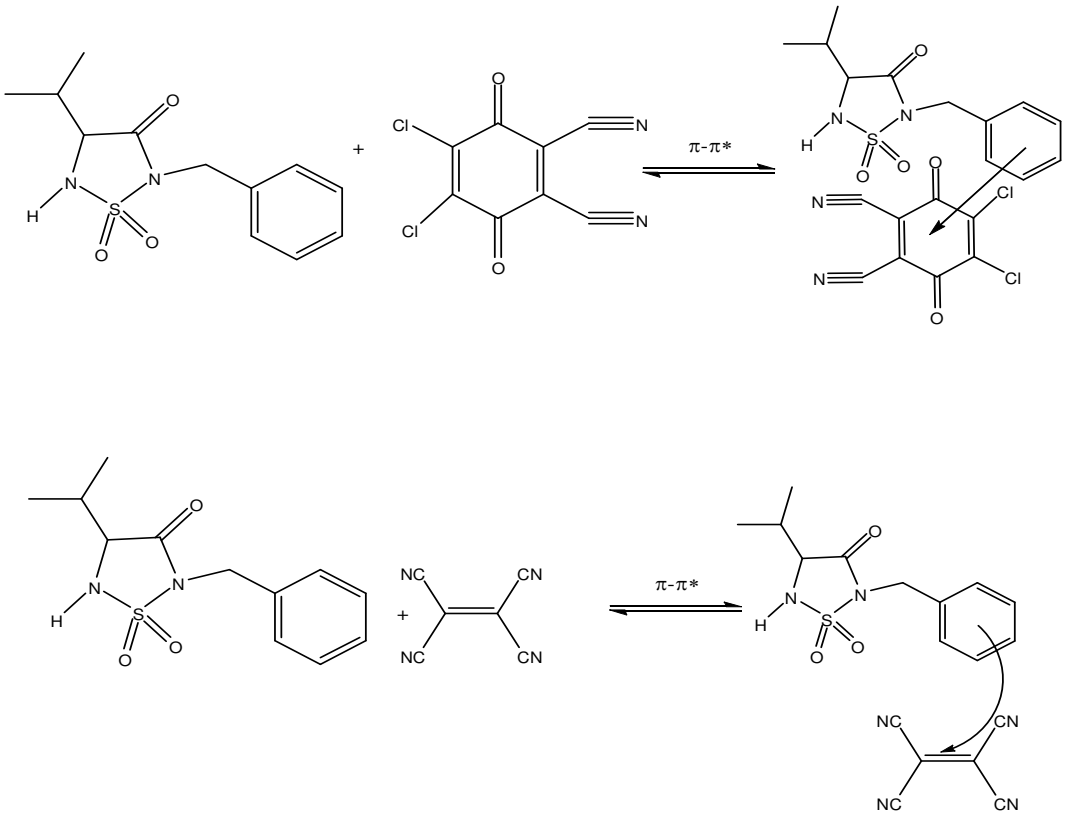

Scheme 1 Mechanism of the CT reaction.

3.8. Molecular modeling studies

In order to gain further insights into the charge transfer process, the experimental study was complemented by quantum chemical calculations on the SF**…**DDQ using Density Functional Theory (DFT) and Time-Dependent Density Functional Theory (TD-DFT) at B3LYP level.

3.8.1 Geometry optimizations and charge distributions

Full-unconstrained geometries optimization of SF, DDQ and their CT-complex in gas phase has been carried out at DFT/ B3LYP/6-311G (d,p) level. The optimization of the complex has been started with two models: with T-shape and parallel geometries according to whether the phenyl ring of SF is placed perpendicularly or in parallel to the DDQ cycle. This last model was found to be the most favorable one. This is justified by the fact that the calculated FT-IR spectrum of the resulting optimized charge transfer complex structure (Fig.10) is in agreement with the experimental one.

New Journal of Chemistry Accepted Manuscript

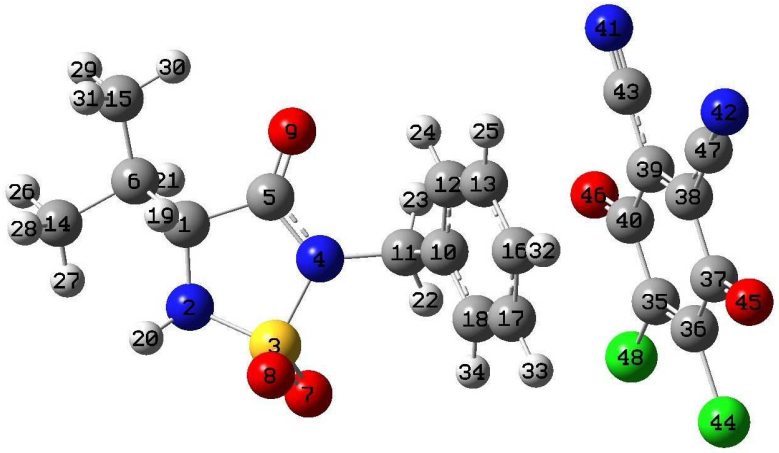

Fig. 10 B3LYP optimized ground state geometric structure of SF**…**DDQ complex.

The calculation of Mulliken atomic charge plays an important role in the application of quantum mechanical calculations to the molecular system because atomic charges affect dipole moment, polarizability, electronic structure, and much more properties of molecular system. As shown in table.6, Mulliken electronic charges on the C1, C2, C4 and C5 atoms in the free DDQ were found to be 0.36, -0.17, 0.36 and 0.01e respectively. But following the complexation with SF, these charges were increased significantly at 1.18, 0.73, 1.30 and 1.31e respectively. In addition, we note that the DDQ moiety is negatively charged. However, the Mulliken charges decreases for most of the atoms on SF, for example, C18, C19, C20 and C21 of the aromatic ring of SF found to be -1.12, -0.17, -0.22 and -0.54 e respectively, decrease upon complexation with DDQ at -0.06, -0.10, -0.06 and -0.09 e respectively. Interestingly, it has been observed that the sum of negative charges, is reduced to SF and increase to DDQ. This indicates that appreciable amount of electronic charge has been transferred from SF to DDQ in SF-DDQ complex.

New Journal of Chemistry Accepted Manuscript

Table 6
Mullken's electronic charge on various atoms of DDQ, SF and SF**…**DDQ complex using DFT (6-311G (d,p) basis set) calculation.

Atom Number	Mullken's electronic charge (a.u.) on different atoms of DDQ	Mullken's electronic charge (a.u.) on different atoms of SF	Mullken's electronic charge (a.u.) on different atoms of SF…DDQ complex
1 C	0.369284		1.185011
2 C	-0.179417		0.734265
3 C	-0.179494		-1.203227
4 C	0.369321		1.307456
5 C	0.011074		1.313523
6 C	0.010992		-1.388971
7 C	0.087957		-0.968193
8 C	0.088083		-0.780788
9 Cl	0.084443		0.133472
10 N		-0.534098	-0.282153
11 S		1.156877	0.642819
12 O		-0.457693	-0.112572
13 O		-0.466989	-0.051263
14 O		-0.348447	-0.212355
15 C		0.510434	-0.270622
16 H		0.171082	0.158239
17 H		0.160946	0.155225
18 C		-1.128331	-0.063264
19 C		-0.174679	-0.105874
20 C		-0.224895	-0.069256
21 C		-0.543220	-0.091045

New Journal of Chemistry Accepted Manuscript

3.8.2 Assignments of vibrational frequencies

The theoretical spectra of the SF**…**DDQ complex were performed with TD-DFT by using B3LYP method with 6-31G(d,p) and 6-311G(d,p) respectively. The comparison with the observed data shows that attempts with the first basis were relatively unsuccessful. However, 6-311G(d,p) bas set seems to give satisfactory results.

For comparison purpose, the observed and simulated FT-IR spectra (B3LYP/6-311(d,p) of the SF**…**DDQ complex are shown in Fig. 11. None of the predicted vibrational spectra has any imaginary frequency.

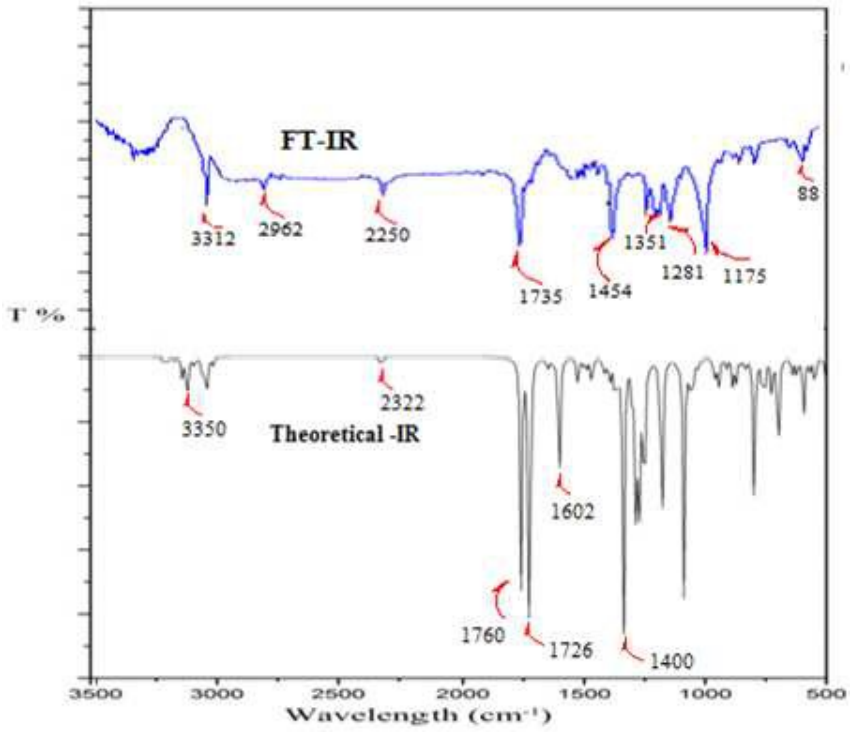

Fig. 11 Observed FT-IR and theoretical spectrum of SF**…**DDQ complex.

A comparative analysis between our experimental and the theoretical spectrum came to the following conclusions:

The characteristic band of (-NH) group of the complex observed at 3312 cm^{-1}, while our theoretical peak is computed at 3550 cm^{-1}. The second experimental assignment show peak at 2250 cm^{-1} is assigned to $\nu_{C\equiv N}$, the correspondent theoretical peak is at 2322 cm^{-1}. The third experimental peak is at 1735 cm^{-1} suggesting a presence of $\nu_{C=O}$, our correspondent

New Journal of Chemistry Accepted Manuscript

theoretical shows two peaks at 1760 and 1726 cm^{-1}. The fourth experimental peak located at 1454 cm^{-1} attributed to $\nu_{C=C}$, was found in theory at 1602 cm^{-1}.

From these foundings, we can conclude that the calculation of the vibrational frequencies is a satisfactory good aid for the assignment of the spectra.

It is worth to mention that, in our calculations, some deviations persist between the observed and calculated wavenumbers due to the neglect of anharmonic effect at the beginning of frequency calculation and of the general tendency of the quantum chemical methods to overestimate the force constants at the exact equilibrium geometry. In the other hand the experiments were performed for solid sample while theoretical ones were calculated in vacuum.

3.8.3 Thermodynamics of complex SF…DDQ in chloroform

The values of thermodynamic parameters such as enthalpy change (ΔH^0), entropy change (ΔS^0) and free energy change (ΔG^0) were calculated by DFT/ B3LYP/6-311G (d,p) at 298.15 K and 1.00 atm pressure and listed in table.7.

Table.7 The statistical thermodynamic calculation of SF **…** DDQ complex in chloroform

Complex	Solvent	ΔG^0 (kJ/mol)	ΔH^0 (kJ/mol)	ΔS^0 (kJ/K.mol)
SF…DDQ	Chloroform	-52.51	-26.25	0.08

With regard to the obtained results from statistical thermodynamic calculation we noticed that the charge-transfer reaction is exothermic, which is in accord with the experimental results

3.8.4 HOMO–LUMO calculations for SF…DDQ complex in both ground and excited states

Molecular orbital can provide insight into the nature of reactivity, and some of the structural and physical properties of molecules. The highest occupied molecular orbital (HOMO) and lowest unoccupied molecular orbital (LUMO), called frontier molecular orbitals (FMO) are the most important orbitals in a molecule. FMO's play important roles in interactions between the molecules as well in electronic spectra of molecule. The energy gap between HOMO and LUMO determines the chemical reactivity, the kinetic stability and the hardness of molecules [49]. In simple molecular orbital theory approaches, the HOMO energy (E_{HOMO}) is related to

New Journal of Chemistry Accepted Manuscript

the ionization energy (IE) by Koopmann's theorem and the LUMO energy (E_{LUMO}) has been used to estimate the electron affinity (EA) [50]. The calculated energy gap of HOMO–LUMO's explains the ultimate charge transfer interface within the molecule. A molecule with a small frontier orbital gap is more polarizable and is generally associated with a high chemical reactivity, low kinetic stability and is also termed as soft molecule [51]. Various HOMOs and LUMOs of SF-DDQ complex in ground state obtained by DFT method at B3LYP 6-311G (d,p) are shown in Fig.12, and the energies of HOMO, HOMO- n, LUMO and LUMO + n, where n = 1–4, for SF, DDQ and SF-DDQ complex in both ground and excited states are provided in Table.8. The HOMO and LUMO energies for SF**…**DDQ complex, based on the optimized structure, were computed at -5.68 and -4.17 ev, respectively. The calculated SF**…**DDQ E_{gap} was 1.51 ev. The lower frontier orbital gap indicates the eventual charge transfer interaction taking place within the complex. In addition, we note from Table 8 that LUMO energy level of the SF**…**DDQ CT complex (-0.153) compares well with the LUMO energy level of DDQ (-0.159), while HOMO energy level (-0.208) of the complex are close to HOMO energy level of SF (-0.211). This tendency for localization of frontier molecular orbitals of SF**…**DDQ system is very much similar to other electron donor–acceptor composites systems [52,53].

TD-DFT/B3LYP/6-311G(d,p) predict one intense electronic transitions at (331 nm) with oscillators strengths $f = 0.0073$ (Table.9), in good agreement with the measured experimental data (λ_{exp}=353nm).

New Journal of Chemistry Accepted Manuscript

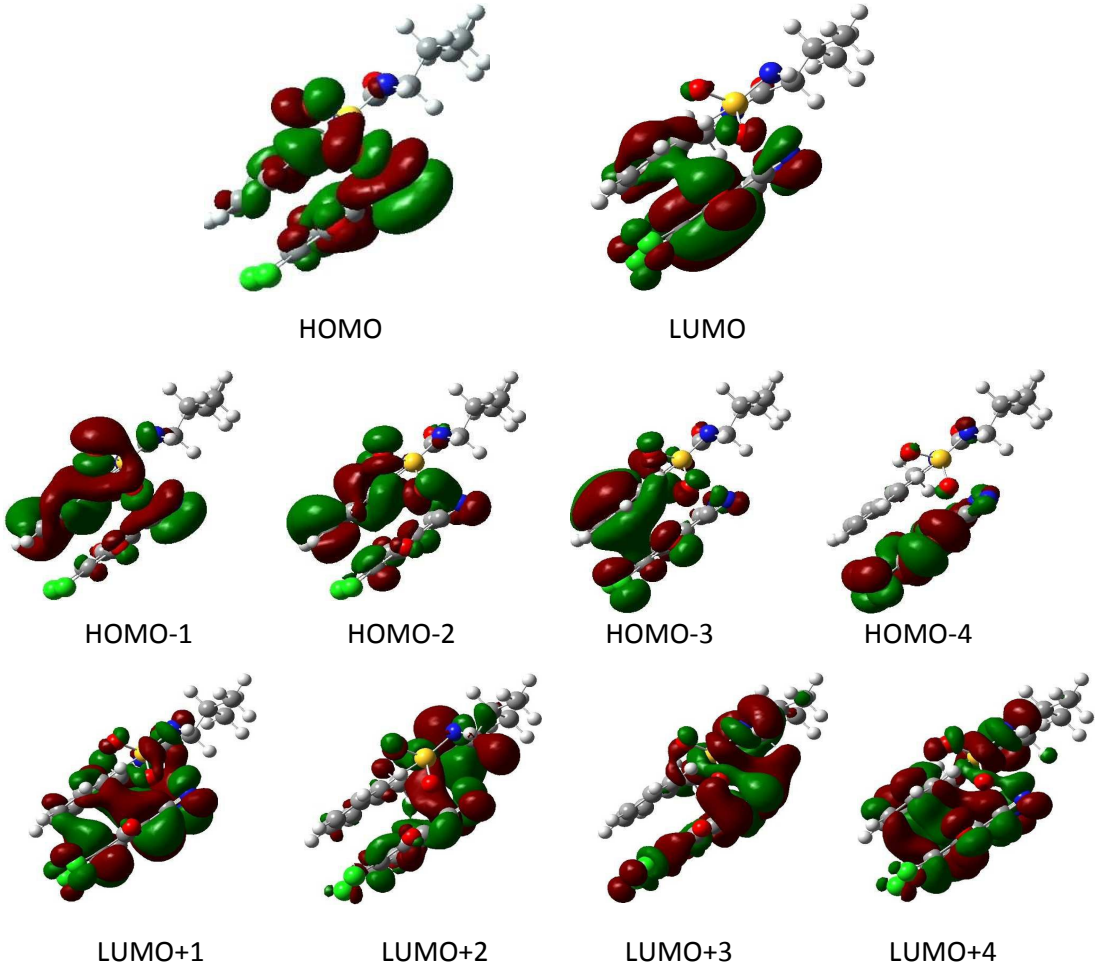

Fig. 12 Frontier molecular orbitals pictures of SF**…**DDQ complex calculated by DFT**.**

New Journal of Chemistry Accepted Manuscript

Table.8 HOMO–LUMO energies for DDQ, SF and SF…DDQ CT complex in ground state.

Name of the orbital	Orbital energy (Hartree)		
	DDQ	SF	SF…DDQ CT Complex
HOMO	-0.304	-0.211	-0.208
HOMO – 1	-0.314	-0.238	-0.245
HOMO – 2	-0.328	-0.250	-0.267
HOMO – 3	-0 .332	-0.293	-0.275
HOMO – 4	-0.350	-0.309	-0.292
HOMO – 5	-0.362	-0.311	-0.295
LUMO	-0.159	-0.045	-0.153
LUMO + 1	-0.112	-0.016	-0.067
LUMO + 2	-0.058	+0.013	-0.057
LUMO + 3	-0.057	+0.029	-0.048
LUMO + 4	-0.027	+0.038	-0.033
LUMO + 5	-0.016	+0.063	-0.030

Table. 9 TD-DFT calculated and experimental wavelengths of SF…DDQ complex.

Transitions occurring	Wavelength (nm)	Oscillator strength	Energy (eV)	Experimental λ_{max}(nm)
HOMO → LUMO + 1	331	0.0073	3.74	353

3.8.5 Molecular electrostatic potential (MEP)

The molecular electrostatic potential (MEP) is best suited for identifying sites for intra- and intermolecular interactions [54]. In drug-receptor, it is a very useful descriptor inunderstanding sites for electrophilic and nucleophilic reactions as well as hydrogen bonding interactions [55]. Different values of the electrostatic potential are represented by different colors: red represents regions of most electro negative electrostatic potential, blue represents regions of most positive electrostatic potential and green represents regions of zero potential. Potential increases in the following order: red < orange < yellow < green < blue. The MEP of DDQ, SF and their SF…DDQ complex have been calculated at B3LYP/6-

New Journal of Chemistry Accepted Manuscript

311G (d,p) level at the optimized geometries shown in Fig. 13. The MEP plot DDQ (Fig. 13b) shows that the positive electrostatic potential (shown in blue) corresponds to the center regions of the six-membered ring with a maximum surface value of 0.07 a.u, while the regions of negative potential(red) are observed around the nitrogen atoms of the cyano groups. For SF moiety, the negative potential (red) shown (Fig. 13a) is mainly associated with the C=O group and positive electrostatic potential (blue) is associated with the N-H (surface value of 0.06 a.u.). When SF electron donor interacts with DDQ (fig. 13c) the center maximum negative value of SF decreases to reach -0.04 a.u. Upon the charge transfer interaction, the NH group of the complex bears positive electron density and can act as a source of H-bond with other neighboring molecules.

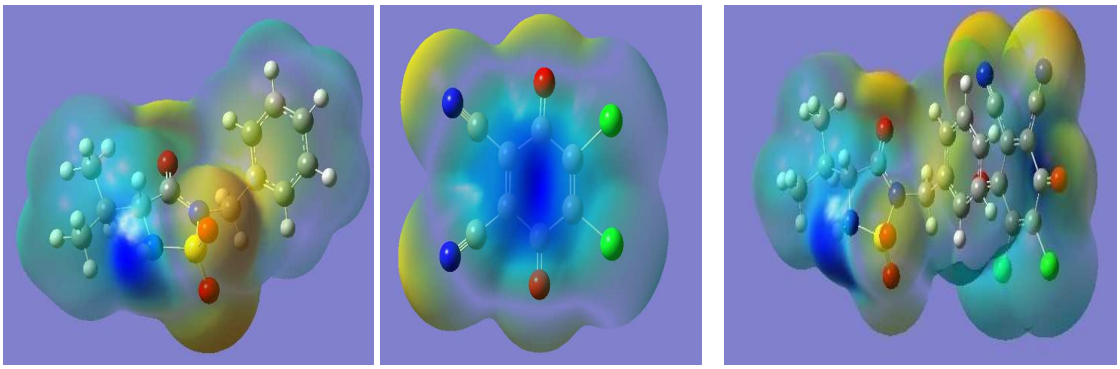

(a) (b) (c)

Fig.13 Molecular electrostatic potential (MEP) maps for (a) SF (b) DDQ and (c) SF**…**DDQ complex in ground state calculated using DFT.

3.8.6 NBO analysis

NBO approach of Weinhold and co-workers [56] has been frequently used in evaluation of intra- and intermolecular interactions, and provides a convenient basis for investigating charge transfer or conjugative interaction in molecular systems. NBO analysis was performed to provide the contribution of atomic orbitals. The electronic wavefunctions are interpreted in term of a set of occupied Lewis orbitals and a set of non-Lewis localized orbitals. The electronic delocalization interaction can be quantitatively described using the stabilization energy ($E^{(2)}$), which is estimated by the second order perturbation theory. This stabilization energy can be expressed as equation (4) [57, 58]:

New Journal of Chemistry Accepted Manuscript

$$E^{(2)} = -n_\sigma \frac{\langle \sigma | F | \sigma \rangle}{\varepsilon_\sigma^* - \varepsilon_\sigma} = -n_\sigma \frac{F_{i,j}^2}{\Delta E} = -n_\sigma \frac{F_{i,j}^2}{E_j - E_i} \quad (4)$$

Where $\langle \sigma | F | \sigma \rangle$ or $F_{i,j}^2$ is the Fock matrix element between the i and j NBO orbitals, $F_{i,j}$ denotes the off-diagonal NBO Fock matrix element. ε_σ^* and ε_σ denote the energies of σ and s^* NBO orbitals, n_σ is the population of the donor s orbital. E_i and E_j denote diagonal elements(orbital energies).

The intermolecular interactions are formed between (C10-C18, C12-C13, C16-C17, C35-C36 and C38-C39) π Bonding orbitals with (C40-O46, C38-C39, C41-C43, C37-O45, C10-C18, C12-C13 and C16-C17) π anti-bonding orbitals, which results charge transfer causing stabilization of the CT complex. The most important interactions in the title complex are: π(C10-C18) with π^* (C40-O46), π(C16-C17) with π^* (C37-O45) and π(C38-C39) with π^* (C16-C17) which give a strong stabilization energies: 4.01, 2.30 and 2.67 kcal/mol, respectively. The other interactions are weak $\pi \rightarrow \pi^*$ charge transfer: π (C12-C13) with π*(C38-C39), π (C12-C13) with π^* (C41-C43), π (C16-C17) with π^* (C38-C39), π (C35-C36) with π^* (C10-C18) and π (C38-C39) with π^* (C12-C13), which donate relatively low stabilization energies (Table 01). Furthermore, there is one $n \rightarrow \pi^*$ established H-bond (O46---H23-C11), which donates a very weak stabilization energy.

3.8.7 NLO property

Organic non-linear optical materials that possess properties such as high non-linear polarizability, high optical damage thresholds, short response time, and a molecular design that is responsive to non-linear optical stimuli, have great potential for use in high-speed integrated optical devices [59]. The first hyperpolarizability (β_0) of a molecular system is calculated using B3LYP/6-311G(d,p) method, based on the finite field approach. The complete equations for calculating the magnitude of the total static dipole moment (μ), mean polarizabilty (α_{tot}) and mean hyperpolarizability (β_o), using the complex from Gaussian 09 output are as follows:

New Journal of Chemistry Accepted Manuscript

$$\mu = \left(\mu_x^2 + \mu_y^2 + \mu_z^2\right)^{1/2}$$

$$\alpha_{tot} = \frac{1}{3}\left(\alpha_{xx} + \alpha_{yy} + \alpha_{zz}\right)$$

$$\Delta\alpha = \frac{1}{\sqrt{2}}\left[\left(\alpha_{xx} - \alpha_{yy}\right)^2 + \left(\alpha_{yy} - \alpha_{zz}\right)^2 + \left(\alpha_{zz} - \alpha_{xx}\right)^2 + 6\left(\alpha_{xy}^2 + \alpha_{yz}^2 + \alpha_{xz}^2\right)\right]^{1/2}$$

$$\beta_0 = \left[\left(\beta_{xxx} + \beta_{xyy} + \beta_{xzz}\right)^2 + \left(\beta_{yyy} + \beta_{yzz} + \beta_{yxx}\right)^2 + \left(\beta_{zzz} + \beta_{zxx} + \beta_{zyy}\right)^2\right]$$

The polarizability and hyperpolarizability are reported in atomic units (a.u), the calculated values have been converted into electrostatic units (e.s.u) (for α: 1 a.u.= 0.1482×10^{-24}esu, for β: 1 a.u. = 8.6393×10^{-33}esu).

The calculated of hyperpolarizability (β_0) and dipole moment (μ) of the compound are 3.74×10^{-30} esu and 3.84 D, respectively [Table 10]. As we compare the hyperpolarizability (β_0) of SF**…**DDQ with urea [60, 61], the value is 8 times greater than that of urea. The high value of hyperpolarizability of the complex SF**…**DDQ is due to the donor and acceptor characteristic of SF and DDQ. The above results show that SF**…**DDQ can be best material for NLO applications

Table.10 The mean polarizability (esu), anisotropy polarizability (esu) and hyperpolarizability (esu) of SF**…**DDQ complex.

NLO behavior	B3LYP 6-311G(d,p)
Mean polarizability (α)	5.30×10^{-23}
Anisotropy of the polarizability (Δα)	25.99×10^{-24}
Hyperpolarizability (β_0)	3.74×10^{-30}

4. Conclusion

Charge-transfer interactions between 4-isopropyl-2-benzyl-1,2,5-thiadiazolidin-3-one1,1-dioxide as electron donor and 2,3-dichloro-5,6-dicyano-1,4-benzoquinone or tetracyanoethylene as π-acceptors were analyzed using spectroscopic techniques. Job's continuous variation method confirmed the formation of 1:1 CT-complexes in methanol and in chloroform at room temperature. The stability constants, K and molar extinction

New Journal of Chemistry Accepted Manuscript

coefficients, ε_{CT} were evaluated by the Benesi–Hildebrand method. The thermodynamic parameters, ΔH^0, ΔS^0 and ΔG^0, were determined by analyzing the variation of lnK with the inverse of the temperature. The values of ionization potentials (I_D), oscillator strengths (f), and transition dipole moment (μ_{EN}) were estimated. The results show that the investigated complexes are stable, exothermic and thermodynamically favored; the thermodynamic parameters were also calculated with the DFT in chloroform, which is in accord with the experimental results. The newly formed complexes were isolated and characterized through FT-IR.

The quantum chemical calculations results with Time-Dependent Density Functional Theory (TD-DFT) at the Becke's three parameter hybrid method with LYP correlation (B3LYP) level reveal that the UV-Vis spectrum and the infrared vibrational frequencies of optimized complex 4-isopropyl-2-benzyl-1,2,5-thiadiazolidin-3-one1,1-dioxide**……**2,3-dichloro5,6dicyano-1,4-benzoquinone were in reasonable agreement with experimental data.

On the other hand, the a results of the calculated of hyperpolarizability show that the complex 4-isopropyl-2-benzyl-1,2,5-thiadiazolidin-3-one 1,1-dioxide**……**2,3-dichloro-5,6dicyano-1,4 benzoquinone can be best material for NLO applications .

The Mulliken charges and the molecular electrostatic potential (MEP) calculations indicate that upon complexation appreciable amount of electronic charge has been transferred from 4-isopropyl-2-benzyl-1,2,5-thiadiazolidin-3-one1,1-dioxide to 2,3-dichloro-5,6dicyano-1,4-benzoquinone and the center maximum negative value of SF decreased while NH group bears positive electron density and can act as a source of H –bond. Natural Bond Orbital (NBO) analysis revealed that the $\pi \rightarrow \pi^*$ interaction gives the strongest stabilization to the system. The calculated results of the complex 4-isopropyl-2-benzyl-1,2,5-thiadiazolidin-3-one1,1-dioxide **…** tetracyanoethylene are similar with the results obtained for the complex 4-isopropyl-2-benzyl-1,2,5-thiadiazolidin-3-one1,1-dioxide**……**2,3-dichloro-5,6dicyano-1,4-benzoquinone

Acknowledgments

The authors would like to acknowledge the Algerian Minister of the High Education and Scientific Research and DGRST for supporting this study through project CNEPRU E015201140082.

New Journal of Chemistry Accepted Manuscript

References

[1] A.G Casado, A.G Campo, Y. Zhang, Xi.Z Pascal and J. Huskens. Polymers, 2013, 5.

[2] S.M. Sondhi, M. Johar, S. Rajvanshi, S.G. Datidar, R. Shukla, R. Raghubir, J.W. Lown, Aust. J. Chem. 54, 2001,169.

[3] M. Kidwai, S. Saxena, S. Rastogi, R. Venkataramanan, Curr. Med. Chem. Anti-Infect. Agents. 2, 2004, 269.

[4] A. Dozal, H. Keyzer, H.K. Kim, W.W. Way, Int. J. Antimicrob. Agents. 14, 2000, 261.

[5] J. Feng, H. Zhong, B.D. Xuebau, Zir. Kexu. 27, 1991,691.

[6] N. Singh, I. M. Khan , A. Ahmad, S. Javed, J. Mol. Liquids. 191, 2014, 142.

[7] J. Feng, H. Zhong, B.D. Xuebau, Zir. Kexu. 27, 1991, 691.

[8] A. Eychmuller, A.L. Rogach, Pure Appl. Chem. 72, 2000, 179.

[9] S.Y. AlQaradawi, H.S. Bazzi, A. Mostafa, E.M. Nour, Spectrochim. Acta A 71, 2008, 1594.

[10] S.M. Teleb, A.S. Gaballa, Spectrochim. Acta A 62, 2005,140.

[11] T. Charan Singh, P. Venkateshwar Rao, T. Veeraiah, G. Venkateswarlu, Indian J. Chem. 42A, 2003, 1666.

[12] M. Shukla, N. Srivastava, S. Saha, J. Mol. Struct. 1021, 2012, 153.

[13] M. Ting, N.J.S. Peters, J. Phys. Chem. A 113, 2009, 11316.

[14] M.S. Refat, H.A. Saad, A.M.A. Adam, J. Mol. Struct. 995, 2011, 116.

[15] E.M. Nour, S.Y. Alqaradawi, A. Mostafa, E. Shams, H.S. Bazzi, J. Mol. Struct. 980, 2010, 218.

[16] E.M. Nour, M.S. Refat, J. Mol. Struct. 994, 2011, 289.

[17] V. Murugesan, M. Saravanabhavan, M. Sekar. Spectrochimica Acta Part A: Molecular and Biomolecular Spectroscopy 147, 2015, 99.

[18] Z. Regaïnia, M. Abdaoui, N. Aouf, G. Dewynter and J. Montero, Tetrahedron, 56, 2000, 381.

[19] W. C. Groutas, R. Kuang, R. Venkataraman, J. B. Epp, S. Ruan, O. Prakash, Biochemistry, 36,1997, 4739.

[20] W. C. Groutas, R. Kuang, S. Ruan, J. B. Epp, R. Venkataraman, T. M. Truong, S. Ruan, Bioorg. Med. Chem, 6, 1998, 661.

[21] W. C. Groutas, R. Kuang, R. Venkataraman, T. M. Truong, Bioorg. Med. Chem. 8, 2000, 1713.

New Journal of Chemistry Accepted Manuscript

[22] L. Ducry, S. Reinelt, P. Seiler, F. Diederich, D. R. Bolin, R. M. Campbell, G. L. Olson, Helv. Chim. Acta, 82, 1999, 2432.

[23] D. Bouchouk, E. Colacino, L. Toupet, N. Aouf, J. Martinez, G. Dewynter, Tetrahedron Letters, 50, 2009, 1100.

[24] G. Dewynter, N. Aouf, M. Criton, J. L Montero,Tetrahedron, 49 ,1993, 65.

[25] E. Black, J. Breed, A. L. Breeze, K. Embrey, R. Garcia, T. W. Gero, L. Godfrey, P. W. Kenny, A. D. Morley, C. A. Minshull, A. D. Pannifer, J. Read, A. Rees, D. J. Russell, D. Toader, J. Tucker, Bioorg. Med. Chem. Lett, 15 ,2005, 2503.

[26] S. Boudjabi, G. Dewynter, N. Voyer, L. Toupet, J. L. Montero, Eur. J. Org. Chem. 1999 ,2275.

[27] S. Mantegani, E. Brambilla, C. Caccia, L. Chiodini, D. Ruggieri, E. Lamberti, E. Di Salle, Salvati, P. Farmaco. 53, 1998, 293.

[28] G. W. Muller, G. E. DuBois, J. Org. Chem. 54, 1989, 4471.

[29] R. R. Crenshaw, A. A. Algieri, US 4394508.

[30] G. Dewynter, N. Aouf, Z. Regainia and J. Montero, Tetrahedron. 52 ,1996, 993.

[31] M.J. Frisch, G.W. Trucks, H.B. Schlegel, G.E. Scuseria, M.A. Robb, J.R. Cheeseman, C.T. Wallingford, Gaussian, Inc, 2009.

[32] A.D. Becke, Phys. Rev. A 38, 1988, 3098.

[33] A.D. Becke, J. Chem. Phys. 96, 1992, 2155.

[34] C. Lee, W. Yang, R.G. Parr, Phys. Rev. B 37, 1988, 785.

[35] R. Ditchfield, W.J. Hehre, J.A. Pople, J. Chem. Phys. 54 ,1971, 724.

[36] P. Job, Ann. Chim. 9, 1928,113.

[37] C. Tablet, I. Matei, M. Hillebrand, InTech, 2012.

[38] H.A. Benesi, J.H. Hildebrand, J. Am. Chem. Soc. 71, 1949, 2703.

[39] P. Douglas, G. Waechter, A. Mills, J. Photochem. Photobiol. A 52, 1990, 473.

[40] M. E. El-Zaria, Spectrochim. Acta A 69, 2008, 216.

[41] R. Foster, T.J. Thomson, Trans. Faraday Soc. 58, 1962, 860.

[42] M.V. Rekharsky, Y. Inoue, Chem. Rev. 98, 1998, 1875.

[43] Y. Inoue, T. Hakushi, Y. Liu, L.H. Tong, B.J. Shen, D.S. Jin, J. Am. Chem. Soc. 115, 1993,475.

[44] G.G. Aloisi, S. Pignataro, J. Chem. Faraday. Trans. 69, 1973, 534.

[45] A.B.P. Leve, Inorganic Electronic Spectroscopy, second ed., Elsevier, Amsterdam, 1985.

[46] E.M. Voigt, C. Reid, J. Am. Chem. Soc. 86 ,1964, 3930.

New Journal of Chemistry Accepted Manuscript

[47] R. Rathore, S.V. Linderman, J.K. Kochi, J. Am. Chem. Soc. 119, 1997, 9393.

[48] R.D. Kross, V.A. Fassel, J. Am. Chem. Soc. 79, 1957, 38.

[49] O. Prasad, L. Sinha, N. Misra, V. Narayan, N, Kumar, J. Pathak, J. Mol. Struct.: Theochem. 940, 2010, 82.

[50] P. Politzer, F. Abu-Awwad, Theor. Chem. Acta. 99, 1998, 83.

[51] I. Fleming, Frontier Orbitals and Organic Chemical Reaction, John Wiley and Sons, New York, 1976.

[52] H. Mizuseki, N. Igarashi, R.V. Belosludov, A.A. Farajian, Y. Kawazoe, Jpn. J. Appl. Phys. 42, 2003, 2503.

[53] H. Mizuseki, N. Igarashi, R.V. Belosludov, A.A. Farajian, Y. Kawazoe, Synth. Met. 138, 2003, 281.

[54] F. Zhang, Y. Zhang, H. Ni, K. Ma, R. Li, Spectrochim. Acta Part A: Mol. Biomol. Spectrosc. 118, 2014, 162.

[55] P. Munshi, T.N. Guru Row, Acta Crystallogr. B62, 2006, 612.

[56] A. Frisch, A.B. Nielson, A.J. Holder, GAUSSVIEW User Manual, Gaussian Inc, Pittsburgh, PA, 2000.

[57] A.E. Reed, L.A. Curtiss, F. Weinhold, Chem. Rev. 88, 1988, 899.

[58] J. Chocholoušová, V. Špirko, P. Hobza, Phys. Chem. Chem. Phys. 6, 2004, 37.

[59] J. Liu, J. Xia, P. Song, Y. Ding, Y. Cui, X. Liu, Y. Dai, and F. Ma, ChemPhysChem, 15, 2014, 2626.

[60] Z.M. Jin, B. Zhao, W. Zhou, Z. Jin, Powder Diff. J, 12, 1997, 47.

[61] S. Savithiri, M. Arockia doss, G. Rajarajan, V. Thanikachalam, J. Mol. Struct, 1105, 2016, 225.

New Journal of Chemistry Accepted Manuscript

We investigated the interaction between sulfahydantoin and two acceptors (DDQ , TCNE) in liquid phase and solid state

Graphical abstract

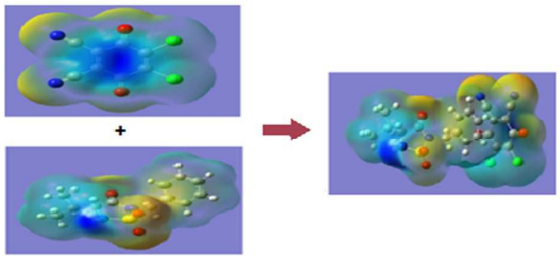

New Journal of Chemistry Accepted Manuscript